Photonic Crystals Made by Holographic Lithography

A.J. Turberfield

Introduction

A photonic crystal is a periodically structured composite material, with a unit cell whose dimensions are of the order of an optical wavelength, made from constituents whose refractive indices differ greatly (Δn is of the order of 2). Three-dimensional (3D) photonic crystals typically consist of interpenetrating networks of dielectric material and air. Holographic lithography[1] is a technology for the fabrication of photonic crystals in which the initial step is to define the 3D microstructure by interference of coherent light in a photosensitive precursor.

The defining characteristic of a photonic crystal is a photonic bandgap, a range of frequencies within which no propagating electromagnetic modes exist.[2] If the bandgap is complete (omnidirectional), then the material acts as an optical insulator. Structural defects in a photonic crystal may give rise to spatially localized electromagnetic modes at energies within the gap:[3] these defect modes are analogous to microcavity-confined modes.[4] Waveguides are formed by coupling defects together.[5] A waveguide operating at a frequency within a photonic bandgap cannot leak—there are no propagating electromagnetic modes in the surrounding photonic crystal capable of carrying energy away. In principle, this allows the fabrication of waveguides that turn corners in a distance of the order of the optical wavelength,[6] requiring 2 orders of magnitude less space than a typical semiconductor ridge waveguide (currently used in integrated optics), which has a minimum bend radius >100 μm. The development of holographic lithography is at least partly motivated by a view of the future of photonic-crystal engineering which sees waveguides operating at frequencies within a photonic bandgap as the basis of miniaturized integrated optical circuits with length scales comparable with those of integrated electronics. Such engineering applications of photonic crystals will require fabrication technologies for the cheap and rapid production of periodic photonic microstructures that have the potential to incorporate engineered structural defects to create microcavities and waveguides.

The relative technological importance of 2D and 3D photonic crystals is still unclear—it seems likely that there will be applications for both. Two-dimensional structures[7] can be created by patterning planar waveguides using well-developed lithographic techniques (including the use of 1D and 2D optical interference patterns to define gratings[8,9]). Two-dimensional photonic crystals allow many aspects of photonic-crystal physics to be demonstrated and exploited. Three-dimensional structures avoid problems created by the out-of-plane diffractive losses suffered by 2D structures; in particular, they will allow the creation of 3D microcavities with quality factors limited only by the intrinsic loss of the dielectric. Three-dimensional photonic crystals are a natural host for 3D optical-device and interconnect architectures.

Some important techniques for the production of 3D photonic crystals are reviewed elsewhere in this issue (see the article by Lin et al.). Colloidal crystals, and structures made by using colloidal crystals as templates,[10–12] are potentially cheap but time-consuming to grow, produce a limited range of structures (and photonic-band structures) and are plagued by unintentional structural defects such as stacking faults; the production of extensive engineered defect structures within a colloidal crystal is difficult. Layer-by-layer growth techniques using VLSI (very large-scale integration) tools[13,14] provide much more control, but require many processing steps and are very expensive. Structures may also be written layer-by-layer by using a tightly focused scanning laser beam to initiate chemical vapor deposition or two-photon photopolymerization;[16,17] resolution is currently limited to micrometer length scales. Holographic lithography, which uses optical interference to define 3D microstructures, is well adapted to the production of structures with submicrometer periodicity. It is a natural extension of conventional optical lithography with the potential to become an industrial process technology that provides the flexibility and control of semiconductor processing but at a much lower cost.

3D Microstructure by Optical Interference

Three-dimensional intensity and polarization distributions may be synthesized by optical interference—as, for example, when a hologram is reconstructed or when a volume hologram is recorded. Periodic patterns are particularly simple and are produced by interference of plane waves. Three-dimensional "optical lattices," in which periodic variations in intensity and polarization create a periodic potential used to trap atoms, are made by interference between laser beams.[18,19] The idea that such an interference pattern could be used to create a periodic pattern of photochemical change as the initial step in the fabrication of a 3D photonic crystal has been proposed independently by more than one group.[1,9,20,21] Two groups have reported the production of a 3D photonic crystal with interpenetrating air and dielectric lattices;[1,21] results of the Ohio State group[1,22] are described in the next section.

The Fourier spectrum of a periodic structure is discrete: it consists of a set of plane waves whose wave vectors are arranged periodically at points of the reciprocal lattice in wave-vector space. The reciprocal lattice determines the real-space lattice of points from which the structure looks the same, that is, the *wave vectors* of the Fourier components determine the translational symmetry of the structure. The *magnitudes* of the Fourier components determine the basis—the contents of the unit cell that is repeated at every lattice point to generate the periodic structure.

A holographic intensity grating generated by interference of n collimated laser beams also has a discrete Fourier

spectrum. Its intensity distribution is given by

$$I(\mathbf{r}) \propto \sum_{l=1}^{n}\sum_{m=1}^{n} \boldsymbol{\varepsilon}_l \cdot \boldsymbol{\varepsilon}_m^* \exp i(\mathbf{k}_l - \mathbf{k}_m)\cdot \mathbf{r}$$

$$\propto \sum_{l=1}^{n}\sum_{m=1}^{n} a_{lm} \exp i\mathbf{G}_{lm}\cdot \mathbf{r}, \qquad (1)$$

where $\mathbf{r}$ is the position vector, $a_{lm} = \boldsymbol{\varepsilon}_l \cdot \boldsymbol{\varepsilon}_m^*$, $\mathbf{G}_{lm} = \mathbf{k}_l - \mathbf{k}_m$, and $\mathbf{k}_m$ and $\boldsymbol{\varepsilon}_m$ are the wave vector and polarization, respectively, of the mth beam. Each Fourier component of the intensity has a wave vector $\mathbf{G}_{lm}$ equal to the difference between two of the laser-beam wave vectors and a magnitude a_{lm} proportional to the scalar product between the polarization vectors of the two beams. If the wave vectors $\mathbf{G}_{lm}$ lie on a lattice in wave-vector space (a reciprocal lattice), then the intensity distribution will have 3D periodicity.

The minimum number of beams required to produce 3D periodicity is four. Interference among *any* four non-coplanar laser beams will produce an intensity grating with 3D periodicity if the differences between their wave vectors is non-coplanar: all Fourier components of the interference pattern necessarily lie on points of a reciprocal lattice whose primitive vectors are the three independent differences between the beam wave vectors. Periodic interference patterns with *any* desired Bravais lattice can be produced by interference of four beams with appropriate wave vectors. Addition of a fifth beam will, in general, produce an incommensurate structure in the interference pattern unless its wave vector is chosen to differ from each of the first four by a reciprocal lattice vector. In other words, five or more laser beams will not, in general, produce a periodic pattern because the wave-vector differences $\mathbf{G}_{lm}$ will not all lie on a reciprocal lattice. The interference pattern also depends on the relative phases of the beams. If the relative phases of four interfering beams vary, then the only effect is to translate the interference pattern.* If more beams are added, then relative phase shifts affect the structure, as well as the position, of the interference pattern.[23] Four is therefore the most convenient number of beams with which to work.

A four-beam interference pattern has 13 Fourier components, of which six are constrained by the condition $a_{lm} = a_{ml}^*$. The magnitudes of these components determine the basis of the interference pattern—that is, the intensity distribution within the unit cell that, repeated at every lattice point, generates the periodic pattern. Equation 1 shows that the magnitudes a_{lm} of the Fourier components are determined by the scalar products of laser polarization vectors. We see that while the wave vectors (i.e., directions and wavelength) of the laser beams determine the translational symmetry of the interference pattern, the shape of the intensity distribution within a unit cell may be controlled by choosing appropriate beam polarizations and intensities. To illustrate this point, Figure 1 shows calculated surfaces of constant intensity[22] in fcc interference patterns produced by interference of four equal-intensity laser beams with wave vectors $\mathbf{k}_1 = \pi/d[201]$, $\mathbf{k}_2 = \pi/d[\bar{2}01]$, $\mathbf{k}_3 = \pi/d[02\bar{1}]$, and $\mathbf{k}_4 = \pi/d[0\bar{2}\bar{1}]$. The difference wave vectors, $\mathbf{k}_2 - \mathbf{k}_1 = 2\pi/d[\bar{2}00]$, $\mathbf{k}_3 - \mathbf{k}_1 = 2\pi/d[\bar{1}1\bar{1}]$, and so on, generate a bcc reciprocal lattice corresponding to a real-space fcc interference pattern with a lattice constant $d = \sqrt{5}\lambda/2 = 397$ nm for a laser wavelength $\lambda = 355$ nm. The two patterns shown in Figure 1 are chosen to illustrate the importance of the choice of laser-beam polarizations. To generate the pattern shown in Figure 1a, polarizations $\boldsymbol{\varepsilon}_i$ were chosen such that $\boldsymbol{\varepsilon}_1 \cdot \boldsymbol{\varepsilon}_2 = \boldsymbol{\varepsilon}_3 \cdot \boldsymbol{\varepsilon}_4 = 0$; all other polarization overlaps were equal. In this case, the Fourier transform of the interference pattern contains nonzero components at the eight $2\pi/d\langle 111\rangle$ reciprocal lattice points only. The primitive basis consists of a cubic "atom" that touches other "atoms" along its edges. Figure 1b shows the effect of rotating the beam polarizations to restore interference between all beams: cuboid "atoms" are connected by "bonds" to eight of their 12 nearest neighbors, making this pattern, unlike the pattern in Figure 1a, suitable for the fabrication of a photonic crystal consisting of connected networks of air and dielectric. An alternative four-beam interference pattern that also generates an fcc structure is described in the following section. This design flexibility gives holographic lithography the potential to create photonic crystals with designed band structures.

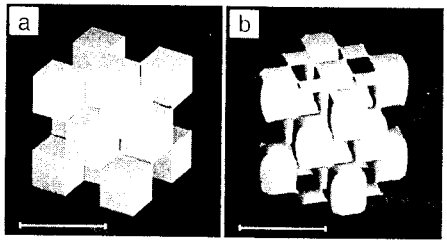

Figure 1. Calculated constant-intensity surfaces in four-beam laser interference patterns with fcc symmetry. The 500-nm scale bars correspond to a laser wavelength of 355 nm; the lattice constant (conventional cube side) is 397 nm. The two patterns shown, (a) and (b), differ only in the choice of laser-beam polarizations, described in the text.

3D Photonic Crystals by Holographic Lithography

3D Structure in a Single Exposure

To create a photonic crystal, a holographic interference pattern must expose a relatively thick film of photoresist. The resist must be nearly transparent, as significant absorption by the resist destroys the periodicity of the interference pattern. This is an unusual constraint: photoresists for conventional lithography are usually highly absorbing to make efficient use of the available photons. In this case, chemical amplification is obligatory—absorption of one photon must initiate the creation (or breaking) of many chemical bonds. We[1,22] use an epoxy-type photoresist based on the resin Epon-SU8[24] with a triaryl sulfonium salt acting as a photoacid generator (PAG). SU8 has low intrinsic absorption at the laser wavelength, is capable of <0.1-μm resolution,[24] and is suitable for the production of structures with high aspect ratios formed from ultrathick films.[24,25] A film of photoresist is spun onto a fused silica disk, and the solvent is evaporated by heating. The film is exposed to the interference pattern generated by four beams split from a single pulse of the Q-switched laser. The duration of the laser pulse (6 ns) is short compared with the time scales of physical and chemical processes induced by the exposure, so the interference pattern is unperturbed by photoinduced changes in the refractive index of the precursor and by mechanical instability of the apparatus. SU8 is a negative photoresist, that is, optical excitation and subsequent processing render it insoluble. Absorption of a UV photon by a molecule of PAG liberates a hydrogen ion; acid-catalyzed polymerization occurs when the film is heated in a post-exposure bake.[24] SU8 has very high functionality with eight epoxy groups per monomer; the network of cross-links formed is therefore potentially very dense, giving high solubility contrast between strongly exposed and weakly exposed material. The photonic-crystal structure is revealed by dissolving weakly exposed material in propylene glycol methyl ether acetate in an ultrasonic bath. The developed film is hard and brittle.

Figure 2 shows the set of four laser wave vectors used in the experiments described in the following. Like the set given

*Changing the phase of beam 1 translates the interference pattern in the direction $\mathbf{G}_{23} \times \mathbf{G}_{34}$, etc.

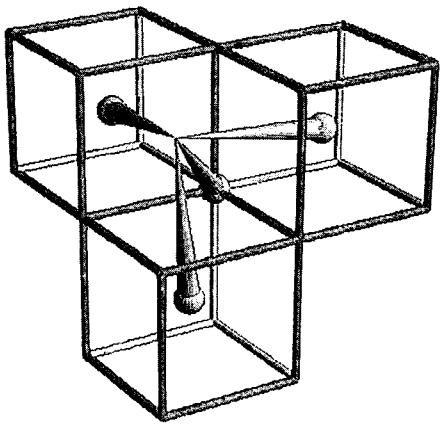

Figure 2. Beam geometry for an fcc interference pattern. The wave vectors of the four laser beams are drawn as cones originating from lattice points in a bcc reciprocal lattice. The differences between the central beam wave vector $\mathbf{k}_1$, which originates from the common point of the three cubes shown, and the three wave vectors $\mathbf{k}_{2-4}$, originating from body-centered lattice points, are the primitive set of reciprocal lattice vectors $2\pi/d\langle\bar{1}11\rangle$.

in the previous section, it also generates an interference pattern with fcc translational symmetry but with a larger unit cell: $d = 3\sqrt{3}\lambda/2 = 922$ nm for laser wavelength $\lambda = 355$ nm. All four wave vectors have equal length (as they must), are drawn originating from points in a bcc reciprocal lattice, and converge to a common point. By construction, therefore, the difference between any pair of wave vectors (a Fourier component of the interference pattern) lies on a bcc reciprocal lattice, ensuring that the real-space interference pattern is fcc.[†] The four wave vectors are $\mathbf{k}_1 = \pi/d[\bar{3}\bar{3}3]$, $\mathbf{k}_2 = \pi/d[5\bar{1}\bar{1}]$, $\mathbf{k}_3 = \pi/d[\bar{1}5\bar{1}]$, and $\mathbf{k}_4 = \pi/d[\bar{1}\bar{1}5]$. Figure 3a shows a calculated surface of constant intensity corresponding to these beam directions.[‡] We calculate that by varying the laser intensity or the sensitivity of the photoresist to adjust the solubility threshold of the resist, this interference pattern can be used to create structures with fully connected polymer and air void lattices having filling fractions in the range of 34–79%. The top surface shown is a close-packed (111) plane, and the repeated *abc* pattern of such planes that makes up an fcc lattice is indicated on the side of the cube. The primitive basis, repeated at each lattice point, is shown as an inset in the figure. The surface has the connectivity of the diamond structure.[2] The basis, which is elongated in the [111] direction, looks like a thick "bond" joining "atoms" at the positions corresponding to those of the two carbon atoms in the diamond basis. Six further "bonds," which again correspond to those in diamond, link the basis to six nearest neighbors, three each in the (111) planes above and below. There are no direct connections between in-plane nearest neighbors.

We have prepared photonic-crystal films consisting of up to 80 close-packed layers by holographic exposure of the photoresist by the interference pattern shown in Figure 3a. They have been characterized by optical[1] and x-ray[27] diffraction. Figure 3b shows a scanning electron microscopy (SEM) image of the surface of one such polymeric photonic crystal. This surface was originally in contact with the optically flat substrate, which was misaligned by 5° from the (111) plane; the broad bands marked *a*, *b*, and *c* that run across the figure correspond to regions where the surface cuts through close-packed layers of the fcc structure. The SEM image therefore contains a large number of closely spaced parallel cross sections through the unit cell, which we stack to reconstruct the 3D structure shown in Figure 3c. The estimated polymer filling

[†] A bcc reciprocal lattice corresponds to an fcc real-space lattice.

[‡] The beam polarizations used in these early experiments are $\boldsymbol{\varepsilon}_1 = [0.81, -0.33, -0.48]$, $\boldsymbol{\varepsilon}_2 = [-0.27, 0.58, 0.77]$, $\boldsymbol{\varepsilon}_3 = [0.80, -0.04, -0.59]$, and $\boldsymbol{\varepsilon}_4 = [0.93, -0.34, -0.12]$. Beam intensities were in the ratio of 5:1:1:1.

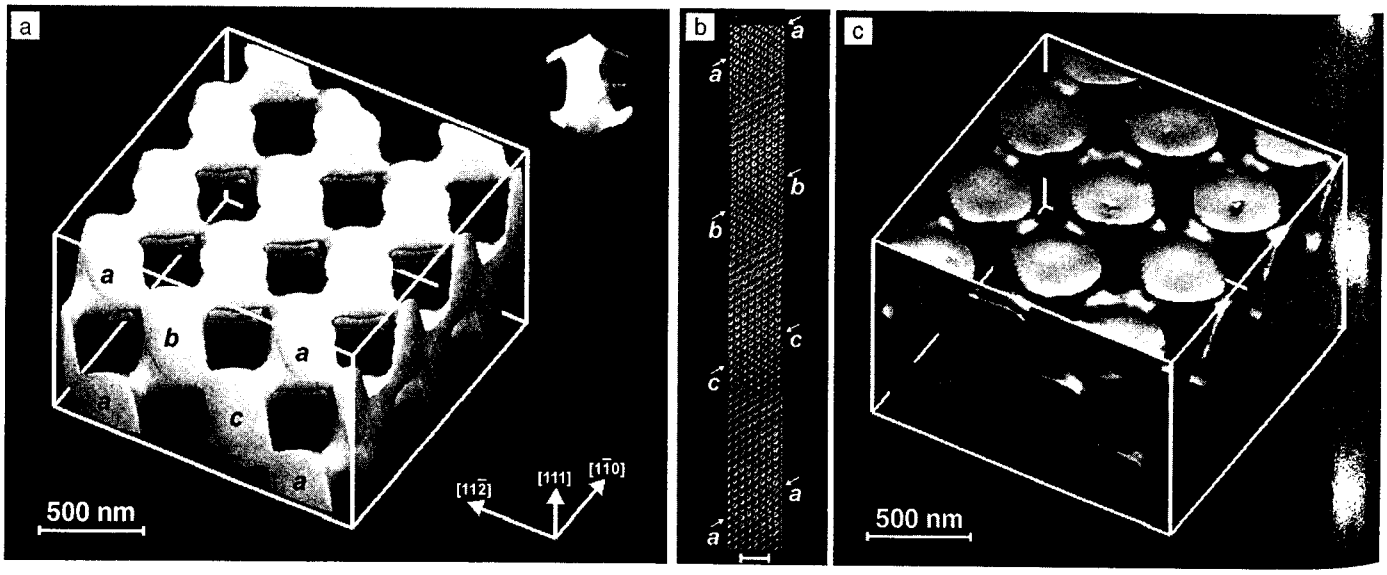

Figure 3. (a) Calculated constant-intensity surface in a four-beam laser interference pattern designed to expose a photoresist in the initial step in the production of an fcc visible optical photonic crystal by holographic lithography. The close-packed layers of the fcc lattice are indicated on one side of the cube. The primitive basis (contents of a Wigner–Seitz unit cell) is shown in the inset. The lattice constant is 922 nm (laser wavelength, 355 nm). (b) Scanning electron microscopy (SEM) image of the bottom surface of a polymeric photonic-crystal film that was initially in contact with the fused silica substrate. The surface is at an angle of ~5° to the (111) plane. Arrows mark regions where the surface cuts through the close-packed planes of the fcc photonic crystal. Scale bar, 2 μm. (c) The reconstructed surface of the photonic crystal.

fraction is 54%. The reconstructed surface of the polymer matrix (Figure 3c) reproduces very closely an intensity contour corresponding to the threshold UV exposure required to convert the photoresist to an insoluble form. The resultant photonic crystal, with its nonspherical basis, resembles an optical frequency version of the microwave structure of Yablonovitch and co-workers.[28]

Figure 4a shows a SEM image of a polymeric photonic crystal. The top surface is a (111) plane; a magnified view is shown in Figure 4d. The film has been fractured to reveal (11$\bar{1}$) cleavage planes. The face-centered structure is stretched in the [111] direction by refraction of the laser beams at the surface of the photoresist; film shrinkage of 10–20% occurs during processing. Figure 4b is a magnified view of another sample showing the (111) top surface and ($\bar{1}$11) and (11$\bar{1}$) cleavage planes. Figure 4c shows a calculated constant-intensity surface that has been cut across narrow "bonds" to mimic the same cleavage planes.

We have demonstrated that our microstructure has adequate connectivity to act as a template for a crystal with higher refractive-index contrast by producing an inverse replica in titania, shown in the SEM image in Figure 4e. The polymeric structure was filled with titanium(IV) ethoxide[11] and heated to 575°C in moist air to burn off the polymer template and sinter the ceramic.

3D Structure by Multiple Exposure

Shoji and Kawata[21] have used a different strategy to create 3D photonic crystals. Instead of using a 3D interference pattern, they used a two-step process, illustrated in Figure 5: three laser beams interfere to create a *two*-dimensional exposure pattern with hexagonal symmetry, and a second set of two beams (not coherent with the first three) interfere to produce a perpendicular *one*-dimensional intensity grating. The intensities of the two interference patterns add; after development, the structure consists of a hexagonal array of rods (defined by the first three beams) divided into sections by perpendicular solid planes (defined by the second two-beam exposure), producing a 3D photonic crystal with a simple hexagonal lattice, as shown in the SEM image of a cross section in Figure 6.[21] In this case, the air spaces do not form a continuous network, so the structure would not be suitable for use as a template.

Chelnokov and co-workers[29] have also proposed a scheme that involves addition of mutually incoherent intensity patterns. They suggest using a four-beam, 3D holographic interference pattern to create repeated exposures; between exposures, the pattern is to be displaced by a fraction of a unit cell by introducing phase shifts between the beams. They propose this as a means of generating a diamondlike structure from an interference pattern that would otherwise produce a "monatomic" fcc structure. Note that the experiments described in this paper demonstrate that it is possible to achieve this result using a single exposure by appropriate selection of beam polarizations and intensities.[1]

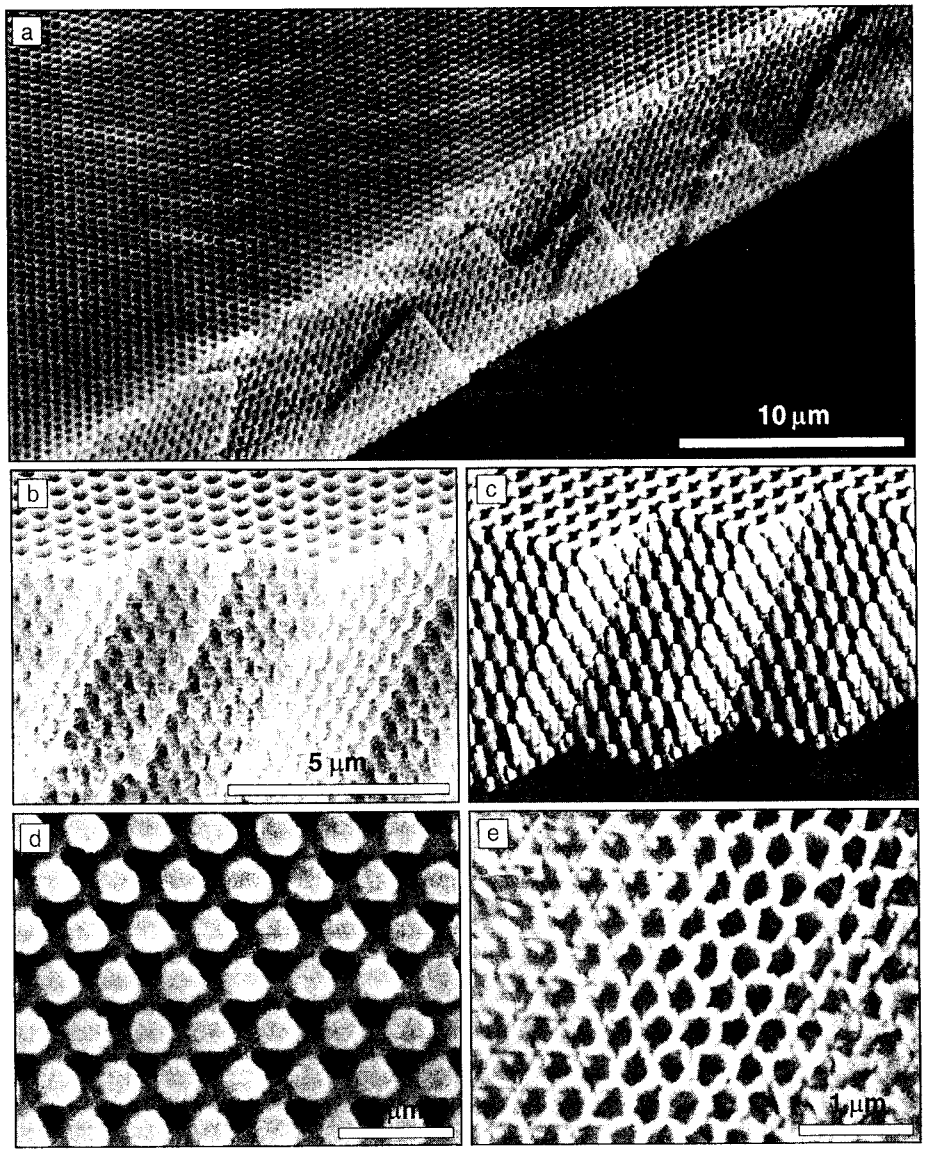

Figure 4. (a) SEM image of an fcc polymeric photonic crystal generated by exposure of a 10-μm film of photoresist to the interference pattern shown in Figure 2. The top surface is a (111) plane; the film has been fractured along (11$\bar{1}$) cleavage planes of the photonic-crystal structure. (b) Close-up of (111) surface and {11$\bar{1}$} cleavage planes. (c) Simulation of (b), formed by cutting a constant-intensity surface along narrow "bonds." (d) Close-up of a (111) surface. (e) Titania photonic crystal with higher refractive-index contrast produced by using the polymeric structure as a template. The surface is slightly tilted from the (111) plane.

Conclusions

Optical lithography, which has a dominant role in the fabrication of submicrometer electronic devices, may be extended to produce 3D microstructures if coherent light is used. A single exposure of a photoresist to a four-beam interference pattern is sufficient to define a photonic-crystal structure that, after development, consists of interpenetrating networks of polymer and air. Photonic crystals with higher refractive-index contrast may be made by

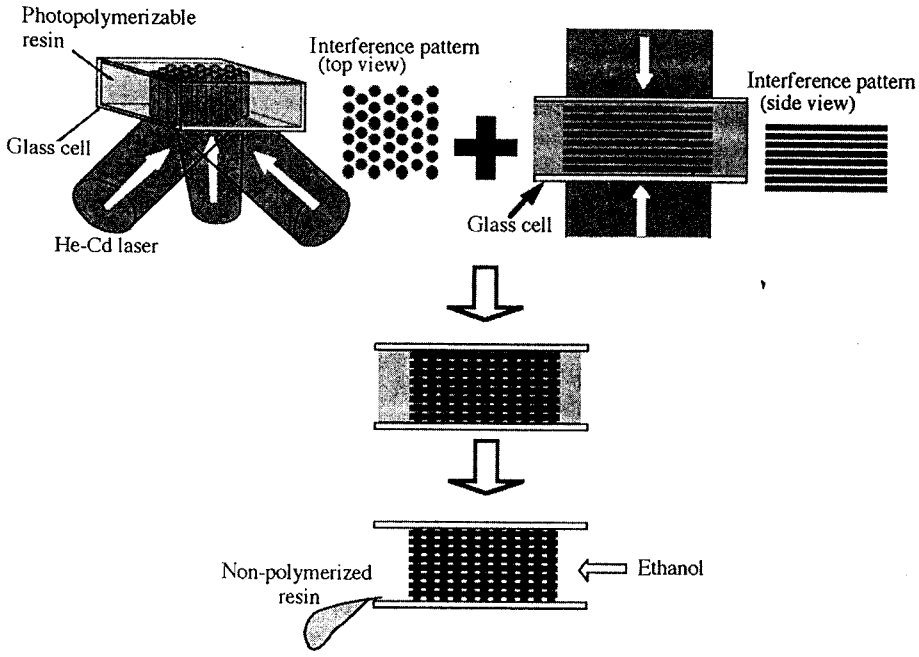

Figure 5. Fabrication of a three-dimensional (3D) hexagonal photonic crystal using 2D and 1D interference patterns (from Reference 21).

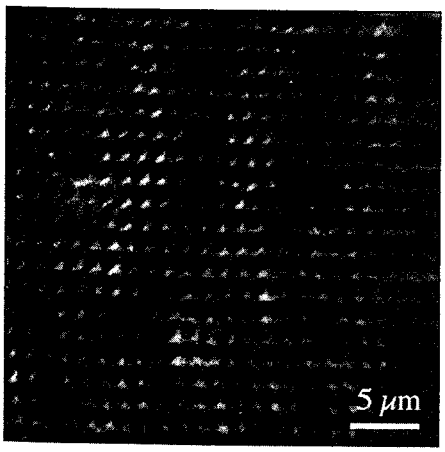

Figure 6. SEM image of a cross section of a hexagonal photonic crystal produced by Shoji and Kawata by the method illustrated in Figure 5 (from Reference 21).

using these polymeric structures as templates. Multiple exposures may also be used to define 3D microstructures; this principle has been demonstrated in experiments that combine 2D and 1D interference patterns to generate a 3D photonic crystal. We note that multiple exposure is a promising route for the addition of defect structures leading to microcavity and waveguide fabrication. Holographic lithography is at an early stage of development, but promises to provide a cheap and flexible route to photonic-crystal fabrication that may eventually be scaled to industrial production.

Acknowledgments

I wish to acknowledge the vital contributions of my colleagues Bob Denning, Mike Harrison, David Sharp, Maya Campbell, and Emma Dedman, without whom none of the experiments presented here would have been possible. I also wish to thank Dr. A.J. Wilkinson and the Department of Materials, University of Oxford, for use of electron microscopy facilities. This work was supported by the EPSRC/MOD/DERA Joint Grant Scheme.

References

1. M. Campbell, D.N. Sharp, M.T. Harrison, R.G. Denning, and A.J. Turberfield, *Nature* **404** (2000) p. 53.
2. E. Yablonovitch, *Phys. Rev. Lett.* **58** (1987) p. 2059.
3. E. Yablonovitch, T.J. Gmitter, R.D. Meade, A.M. Rappe, K.D. Brommer, and J.D. Joannopoulos, *Phys. Rev. Lett.* **67** (1991) p. 3380.
4. J.S. Foresi, P.R. Villeneuve, J. Ferrara, E.R. Thoen, G. Steinmeyer, S. Fan, J.D. Joannopoulos, L.C. Kimmerling, H.I. Smith, and E.P. I[illegible]n, *Nature* **390** (1997) p. 143.
5. S.-Y. Lin, E. Chow, V. Hietala, P.R. Villeneuve, and J.D. Joannopoulos, *Science* **282** (1998) p. 274.
6. A. Mekis, J.C. Chen, I. Kurland, S. Fan, P.R. Villeneuve, and J.D. Joannopoulos, *Phys. Rev. Lett.* **77** (1996) p. 3787.
7. T.F. Krauss and R. De La Rue, *Prog. Quantum Electron.* **23** (1999) p. 51.
8. S.C. Kitson, W.L. Barnes, and J.R. Sambles, *IEEE Photon. Technol. Lett.* **8** (1996) p. 1662
9. V. Berger, O. Gauthier-Lafaye, and E. C[illegible]rd, *J. Appl. Phys.* **82** (1997) p. 60.
10. A.M. Kapitonov, N.V. Gaponenko, V.N. Bogomolov, A.V. Prokofiev, S.M. Samoilovich, and S.V. Gaponenko, *Phys. Status Solidi A* **165** (1998) p. 119.
11. B.T. Holland, C.F. Blanford, and A. Stein, *Science* **281** (1998) p. 538.
12. J.E.G.J. Wijnhoven and W.L. Vos, *Science* **281** (1998) p. 802.
13. S. Noda, N. Yamamoto, and A. Sasa[illegible]m, *J. Appl. Phys., Part 2: Lett.* **35** (1996) p. L909.
14. J.G. Fleming and S.-Y. Lin, *Opt. Lett.* **24** (1999) p. 49.
15. M.C. Wanke, O. Lehmann, K. Müller, Q.Z. Wen, and M. Stuke, *Science* **275** (1997) p. 1284.
16. B.H. Cumpston, S.P. Ananthavel, S. Barlow, D.L. Dyer, J.E. Ehrlich, L.L. Erskine, A.A. Heikal, S.M. Kuebler, I.-Y.S. Lee, D. McCord-Maughon, J.Q. Qin, H. Röckel, M. Rumi, X.-L. W[illegible] R. Marder, and J.W. Perry, *Nature* **398** (1999[illegible]51.
17. H.-B. Sun, S. Matsuo, and H. Misawa, *Appl. Phys. Lett.* **74** (1999) p. 786.
18. G. Grynberg, B. Lounis, P. Verkerk, J.-Y. Courtois, and C. Salomon, *Phys. Rev. Lett.* **70** (1993) p. 2249.
19. A. Hemmerich, C. Zimmermann, and T.W. Hänsch, *Europhys. Lett.* **22** (1994) p. 89.
20. Z. Jakšić and Z. Djinović, in *Proc. XLI Yugoslav Conf. ETRAN*, Vol. 4, *Vrnjačka [illegible]ija, Serbia* (1998) p. 27.
21. S. Shoji and S. Kawata, *Appl. Phys. Lett.* **76** (2000) p. 2668.
22. D.N. Sharp, M. Campbell, E.R. Dedman, M.T. Harrison, R.G. Denning, and A.J. Turberfield, "Photonic Crystals for the Visible Spectrum by Holographic Lithography," *Opt. Quantum Electron.* in press.
23. K.I. Petsas, A.B. Coates, and G. Grynberg, *Phys. Rev. A* **50** (1994) p. 5173.
24. K.Y. Lee, N. LaBianca, S.A. Risht[illegible] S. Zolgharnain, J.D. Gelorme, J. Shaw, and T.H.P. Chang, *J. Vac. Sci. Technol., B* **13** (1995) p. 3012.
25. H. Lorenz, M. Despont, N. Fahrni, N. LaBianca, P. Renaud, and P. Vettiger, *J. Micromech. Microeng.* **7** (1997) p. 121; H. Lorenz, M. Despont, N. Fahrni, J. Brugger, P. Vettiger, and P. Renaud, *Sens. Actuators, A, Phys.* **64** (1998) p. 33
26. C.T. Chan, S. Datta, K.M. Ho, and C.M. Soukoulis, *Phys. Rev. B* **50** (1994) p. 1988
27. D.N. Sharp, R.G. Denning, M. Ca[illegible]ell, and A.J. Turberfield (unpublished manuscript).
28. E. Yablonovitch, T.J. Gmitter, and K.M. Leung, *Phys. Rev. Lett.* **67** (1991) p. 2295.
29. A. Chelnokov, S. Rowson, J.-M. Lourtioz, V. Berger, and J.-Y. Courtois, *J. Opt. A* **1** (1999) p. L3